DMD Fast Forward. Published on July 25, 2013 as doi:10.1124/dmd.113.053108

The Effect of Ritonavir on Human CYP2B6 Catalytic Activity: Heme Modification Contributes to the Mechanism-Based Inactivation of CYP2B6 and CYP3A4 by Ritonavir

Hsia-lien Lin, Jaime D'Agostino, Cesar Kenaan,

Diane Calinski, and Paul F. Hollenberg

Department of Pharmacology, University of Michigan, Ann Arbor, Michigan 48109

DMD Fast Forward. Published on July 25, 2013 as DOI: 10.1124/dmd.113.053108
This article has not been copyedited and formatted. The final version may differ from this version.

Running title: Inactivation of 2B6 and 3A4 by Ritonavir

To whom correspondence should be addressed: Paul F. Hollenberg, Department of Pharmacology, 2301 MSRB III, 1150 West Medical Center Drive, Ann Arbor, MI 48109-5632.

Phone: (734) 764-8166. Fax: (734) 763-5378.

E-mail: phollen@umich.edu

Number of text pages: 41

Number of Tables: 1

Number of Figures: 10

Number of References: 51

Number of words in the Abstract: 231

Number of words In the Introduction: 715

Number of words in the Discussion: 1464

Abbreviations: CYP2B6, human cytochrome P450 2B6; RTV, ritonavir; PI, protease inhibitor; GSH, glutathione; CPR, NADPH-cytochrome P450 reductase;

TFA, trifluoroacetic acid; EFC, 7-ethoxy-4-(trifluoromethyl)coumarin;

BFC, 7-benzyloxy-4-(trifluoromethyl)coumarin;

HFC, 7-hydroxy-4-(trifluoromethyl)coumarin; HPLC, high pressure liquid chromatography; ESI, electrospray ionization; LC-MS, liquid chromatography-mass spectrometry; LC-MS/MS, liquid chromatography-tandem mass spectrometry;

K_s, spectral dissociation constant.

DMD Fast Forward. Published on July 25, 2013 as DOI: 10.1124/dmd.113.053108
This article has not been copyedited and formatted. The final version may differ from this version.

Abstract

The mechanism-based inactivation of human CYP2B6 by ritonavir (RTV) in a reconstituted system was investigated. The inactivation is time-, concentration- and NADPH-dependent and exhibits a K_I of 0.9 μM, a k_{inact} of 0.05 min^{-1} and a partition ratio of ~3. Liquid chromatography-tandem mass spectrometry (LC-MS/MS) analysis showed that the protonated molecular ion of RTV exhibits an *m/z* at 721 and its two major metabolites are an oxidation product with MH^+ at *m/z* 737 and a decarbamoylated product with MH^+ at *m/z* 580. Inactivation of CYP2B6 by incubation with 10 μM RTV for 10 min resulted in ~50% loss of catalytic activity and native heme, but no modification of the apoprotein was observed. RTV was found to be a potent mixed-type reversible inhibitor (K_i = 0.33 μM) and a type II ligand (K_s = 0.85 μM) of CYP2B6. Although previous studies have demonstrated that RTV is a potent mechanism-based inactivator of CYP3A4, the molecular mechanism responsible for the inactivation has not been determined. Here, we provide evidence that RTV-inactivation of CYP3A4 is due to heme destruction with the formation of a heme-protein adduct. Similar to CYP2B6, there is no significant modification of the apoprotein. Furthermore, LC-MS/MS analysis revealed that both CYP3A4 and human liver microsomes form an RTV-GSH conjugate having a MH^+ at *m/z* 858 during metabolism of RTV, suggesting the formation of an isocyanate intermediate leading to formation of the conjugate.

Introduction

Four protease inhibitors (PI), saquinavir, indinavir, nelfinavir and ritonavir (RTV), were licensed for use from 1995-1997 for treating HIV-infected patients resulting in a significant decline in the morbidity and mortality among patients with advanced HIV infections (Palella et al., 1998; Hull and Montaner, 2011). However, due to toxicity issues and adverse reactions including metabolic abnormalities, increased cardiovascular risk, and drug-drug interactions, the use of high dose RTV monotherapy is no longer recommended (Piscitelli et al., 1996). RTV was found to be a potent reversible inhibitor and also a mechanism-based inactivator of human liver and intestinal microsomal drug metabolism and of expressed CYP3A4 (Kumar et al., 1996; Koudriakova et al., 1998; von Moltke et al., 2000; Ernest et al., 2005). RTV is currently used at low doses in combination with other PIs such as lopinavir, amprenavir, and saquinavir in order to inactivate or inhibit CYP3A4 and "pharmacologically boost" the bioavailability of other PIs (Kempf et al., 1997; Zeldin and Petruschke, 2004; Hull and Montaner, 2011). Although relatively low doses (100-300 mg) of RTV are used, the concentration of RTV in plasma can reach more than 10 μM. Therefore, the interaction of RTV with other substrates/drugs primarily metabolized by CYP3A4 and other CYPs still needs to be evaluated (Foisy et al., 2008; Daali et al., 2011; Kirby et al., 2011a; Kirby et al., 2011b).

Besides affecting CYP3A4 drug metabolism, RTV has been shown to interact with other CYPs including 2C9, 2D6, 3A5 and 3A7 (Kumar et al., 1996; Koudriakova et

al., 1998; von Moltke et al., 1998; Granfors et al., 2006). Inhibition of CYP2B6-catalyzed bupropion hydroxylation by RTV has been reported in human liver microsomes (Hesse et al., 2001). Recently, using recombinant human supersomes and specific inhibitors of CYPs, RTV was shown to inhibit CYP2B6-catalyzed bioactivation of prasugrel (Daali et al., 2011). Co-administration of drugs is common during the treatment of HIV-positive patients. For instance, studies estimate that depression affects 32% to 56% of HIV-positive persons and more than 10% of the deaths in HIV-infected patients are due to cardiovascular diseases (Ferrando et al., 1997; Sabin et al., 2008). Since bupropion is often used for the treatment of depression, and prasugrel is used for the prevention of acute coronary syndromes in HIV-infected patients, the potential for drug-drug interactions may not be limited to substrates for the CYP3A subfamily of P450s alone and should be evaluated for drugs preferentially metabolized by CYP2B6 (Avants et al., 1998; Turpeinen et al., 2006; Wang and Tompkins, 2008; Duggan and Keating, 2009). CYP2B6 is expressed in human liver, intestine, brain, kidney and lung and exhibits significant genetic polymorphisms (Gervot et al., 1999; Lang et al., 2001; Zanger et al., 2007). The expression of CYP2B6 varies as much as 200-fold, and the relative contribution of CYP2B6 to total hepatic CYP content ranges from 2 to 10% (Turpeinen et al., 2006; Wang and Tompkins, 2008).

In this study, we used a reconstituted system consisting of expressed CYP2B6 and NADPH-cytochrome P450 reductase (CPR) to investigate: 1) metabolism of RTV by CYP2B6; 2) the kinetic values for mechanism-based inactivation of CYP2B6 by RTV using 7-ethoxy-4-fluoromethylcoumarin (EFC) *O*-deethylation as the probe substrate; 3)

the two possible mechanisms of CYP2B6 inactivation by RTV due to either heme loss or covalent modification of the apoprotein as determined by high pressure liquid chromatography (HPLC) and ESI-LC-MS, respectively; 4) the spectral dissociation constant (K_s) for binding of RTV to CYP2B6; 5) the partition ratio for mechanism-based inactivation; and 6) the formation of a GSH conjugate with the reactive intermediate of RTV.

Although RTV is one of the most potent mechanism-based inactivators of CYP3A4, and the crystal structures of the complex between CYP3A4 and RTV and its analogs are available, the contributions of heme and/or apoprotein modification to the loss of catalytic activity during mechanism-based inactivation has not been determined (Koudriakova et al., 1998; von Moltke et al., 2000; Ernest et al., 2005; Sevrioukova and Poulos, 2010; Sevrioukova and Poulos, 2012). Using essentially the same procedures as in the CYP2B6 studies described above, 7-benzyloxy-4-(trifluoromethyl)coumarin (BFC), a substrate of CYP3A4, was used as a probe to re-evaluate the mechanism-based inactivation of CYP3A4 by RTV in a reconstituted system. Here, also we observed that the inactivation of CYP3A4 by RTV is due to heme destruction accompanied by the formation of a heme-protein adduct.

Materials and Methods

Chemicals. NADPH, GSH, and catalase were purchased from Sigma-Aldrich (St. Louis, MO). EFC was from Invitrogen Corp. (Carlsbad, CA). BFC and human liver microsomes were from BD Biosciences (Franklin Lakes, NJ). 7-Hydroxy-4-(trifluoromethyl)coumarin (HFC) was from Oakwood Products, Inc. (West Columbia, SC). RTV was from Toronto Research Chemicals (North York, ON). All other chemicals and solvents were of the highest purity available from commercial sources.

Enzyme Assay and Inactivation of the P450s. CYP2B6, CYP3A4 and CPR were expressed in *Escherichia coli* TOPP3 cells and purified according to previous published procedures (Scott et al., 2001). To assess catalytic activity, the purified CYP2B6 and CPR were reconstituted at 22ºC for 30 min as described previously (Lin et al., 2009). The primary reaction mixture contained 0.5 nmol P450, 1 nmol reductase, 2 mM GSH, 100 units of catalase, and RTV (0.5 to 20 μM) in 500 μl of 100 mM potassium phosphate buffer (pH 7.7). After incubation of the primary reaction in the presence of 1 mM NADPH at 22ºC with RTV for the time indicated (6 to18 min), a 3 μl aliquot was removed and added to 300 μl of a secondary reaction mixture containing 50 μM EFC and 200 μM NADPH for 10 min. Similar methods were applied for CYP3A4 catalytic activity except BFC was the substrate and the incubations were at 37ºC (Lin and Hollenberg, 2007). The formation of HFC, the product from EFC metabolized by CYP2B6 and from BFC metabolized by CYP3A4, was determined using a fluorescence plate reader (with excitation at 410 nm and emission at 510 nm) on a Wallace Victor II

1420-042 multilabel counter (PerkinElmer, Shelton, CT). Calculations of the kinetic values for mechanism-based inactivation were performed as previously described (Zhang et al., 2009).

Determination of the Partition Ratio. RTV at concentrations ranging from 0.1 to 100 μM was added to the primary reaction mixtures containing 1 μM CYP2B6 or CYP3A4. The reactions were initiated by the addition of 1 mM NADPH and incubated for 30 min in order to allow the inactivation to go to completion (Silverman, 1996). Aliquots were removed and assayed for residual catalytic activity as described above.

HPLC Analysis of the Heme. An HPLC system with a Waters 600E system controller was used to investigate the loss of native heme and the formation of heme adducts. Aliquots containing 100 pmol of control (-NADPH) or inactivated (+NADPH) P450, were incubated with 10 μM RTV (CYP2B6) or 2 μM RTV (CYP3A4) for 10 min as described above to allow for inactivation and then were analyzed using a C4 reverse-phase column (5 μm, 4.6 x 250 mm, 300 Å; Phenomenex, Torrance, CA). The solvent system consisted of solvent A (0.1% trifluoroacetic acid [TFA] in water) and solvent B (0.05% TFA in acetonitrile). The column was eluted with a linear gradient from 30% to 80% B over 30 min at a flow rate of 1 ml/min and the column eluent was monitored at 400 nm using a model 996 photodiode-array Detector (Millipore Corporation, Bilerica, MA).

DMD Fast Forward. Published on July 25, 2013 as DOI: 10.1124/dmd.113.053108
This article has not been copyedited and formatted. The final version may differ from this version.

ESI-LC-MS Analysis of the Apoprotein. Control and inactivated samples incubated with 10 μM RTV for 10 min were prepared as described above. Aliquots containing 50 pmol of P450 were analyzed on a C3 reverse-phase column (Zorbax 300SB-C3, 3.5 μm, 3.0 x 150 mm; Agilent Technologies, Santa Clara, CA) equilibrated with 40% acetonitrile and 0.1% TFA at a flow rate 0.3 ml/min. After 5 min, the column effluent was directed into the mass analyzer of a LCQ mass spectrometer (Thermo Fisher Scientific, San Jose, CA) as described previously (Kent et al., 2006). The acetonitrile concentration was increased linearly to 90% over the next 25 min in order to separate the components of the reconstitution mixture and the mass spectra were recorded. The spectra corresponding to the protein envelopes for the P450s were deconvoluted to give the masses associated with each protein envelope using the Bioworks software package (Thermo Fisher Scientific). The ESI source conditions were: sheath gas set at 90 arbitrary units, the auxiliary gas was set at 30 arbitrary units, the spray voltage was 4.2 kV, and the capillary temperature was 230°C.

Spectral Binding of RTV to CYP2B6. For the binding of RTV to CYP2B6, the K_s was determined by difference spectroscopy on a Shimadzu 2501 spectrophotometer (Kyoto, Japan). Equal volumes of 1 μM solutions of CYP2B6 were aliquoted into the reference and sample cuvettes and the baseline recorded. The difference in the absorbance was recorded from 370 to 600 nm after the addition of a series of aliquots of RTV in methanol to the sample cuvette with the same amount of methanol being added to the reference cuvette. The differences in the absorbances between ~428 nm and ~405 nm at various

concentrations of added RTV (0.1 to 20 μM) were fitted with the Michaelis-Menten equation using GraphPad Prism5 software (San Diego, CA) to obtain the K_s value.

Reversible Inhibition of CYP2B6 by RTV. For the studies on the reversible inhibition by RTV, various concentrations of EFC (1, 2.5, 5, 10, 25 and 50 μM) were prepared and incubated with increasing concentrations of RTV (0, 0.1, 0.3, 0.6 and 1 μM) for 5 min and then the reactions were initiated by adding 200 μM NADPH and the HFC product was measured fluorometrically as described. The kinetic parameters, K_m and k_{cat}, were fitted using the Michaelis-Menten equation and the K_i was obtained by global fitting to a mixed-model inhibition equation using GraphPad Prism5 software (San Diego, CA).

LC-MS/MS Analysis of Metabolites and the GSH Conjugate Formed during Metabolism of RTV. Samples containing 250 pmol of CYP2B6, CYP3A4, or 3 mg of human liver microsomes in 250 μl reaction mixtures were prepared as described above. The samples were incubated with 40 μM RTV with/without 1 mM NADPH at 37°C for 20 min and then the reactions were terminated by the addition of 1 ml of acetonitrile. The mixtures were centrifuged at 13,200 g at room temperature for 10 min. The supernatants were dried under N_2 gas and re-suspended in 100 μl of 50% methanol. The samples were analyzed on a C18 reverse-phase column (Luna, 3 μm, 4.6 x 100 mm, Phenomenex, Torrance, CA) with solvent A (0.1% acetic acid/water) and solvent B (0.1% acetic acid/acetonitrile). A gradient of 30% B for 5 min followed by a gradient to 40% B over 15 min and then increasing linearly to 90% B over 15 min at a flow rate of 0.3 ml/min

was used. The column effluent was directed into the ESI source of a LCQ mass spectrometer (Thermo Fisher Scientific). The ESI conditions were: sheath gas flow rate, 90 arbitrary units; auxiliary gas, 30 arbitrary units; spray voltage, 4.5 kV; capillary temperature, 170°C; capillary voltage, 30 V; and tube lens offset, 25 V. Data were acquired in positive ion mode using Xcalibur software (Thermo Fisher Scientific) with one full scan followed by two data-dependent scans of the most intense and the second most intense ions.

Results

Identification of the Metabolites of RTV by LC-MS/MS Analysis. The major metabolites of RTV produced by human liver microsomes and expressed CYP3A4 have previously been reported (Kumar et al., 1996; Koudriakova et al., 1998). The major metabolites formed by CYP2B6 and CYP3A4 formed in a reconstituted systems were characterized and compared in the present study (Fig. 1). The extracted ion chromatogram for the protonated molecular ion of RTV is at *m/z* 721, which eluted at 33 min. For CYP3A4, four ions with *m/z* values of 580, 582, 737, and 707, corresponding to metabolites a, b, c, and d, respectively, were observed. For CYP2B6, metabolites a and c were observed. The MS/MS spectrum for each of these precursor ions is displayed in Fig. 2. The four metabolites of RTV and the major fragment ions of each metabolite are in agreement with previous studies (Kumar et al., 1996; Koudriakova et al., 1998). The chemical structures of the four metabolites and RTV as well as the sites of fragmentation are displayed in Fig. 3. Metabolite a (*m/z* 580) is from deacylation of RTV, metabolite b (*m/z* 582) is from *N*-dealkylation of RTV, metabolite c (*m/z* 737) is from hydroxylation at the isopropyl side chain of RTV, and metabolite d (*m/z* 707) is from *N*-demethylation of RTV.

Kinetic Values for the Inactivation of CYP2B6 by RTV. The inactivation of the CYP2B6-catalyzed EFC deethylation by RTV was measured using various concentrations of RTV and various time points for each concentration. As shown in Fig. 4A, the inactivation of CYP2B6 was time- and concentration-dependent and required

NADPH. Linear regression analysis of the time course data was used to estimate the initial rate constants (k_{obs}) for the inactivation of CYP2B6 by the various concentration of RTV. The kinetic values were obtained by fitting the k_{obs} values at the various concentrations of RTV to the Michaelis-Mention equation (GraphPad Prism 5). The K_I, k_{inact},and $t_{1/2}$ were determined to be 0.9 μM, 0.05 min^{-1}, and 15 min, respectively (Fig. 4B). These results indicate that RTV is a mechanism-based inactivator of CYP2B6.

Partition Ratio for the Inactivation of CYP2B6 or CYP3A4 by RTV. CYP2B6 or CYP3A4 was incubated with various concentrations of RTV for 30 min in order for the inactivation to reach completion. The percentage of activity remaining was plotted as a function of the molar ratio of inactivator to P450 (Fig. 4C). The partition ratio was estimated from the intercept of the linear regression line obtained from the lower ratios of RTV to P450 with the straight line derived from higher ratios of RTV to P450. Using this method, the partition ratio was estimated to be ~3 for CYP2B6 (Fig. 4C) and ~1 for CYP3A4 (data not shown).

Reversible Inhibition of CYP2B6 EFC Deethylation Activity by RTV. Using EFC at varying concentrations (1 to 50 μM) as a substrate, the rates of HFC formation were determined in the presence of various concentrations of RTV (0 to 1 μM) (Fig. 5A). The K_m and k_{cat} values were determined from the data in Fig. 5A by fitting to the Michaelis-Menten equation using GraphPad Prism5 software and, as shown in Table 1, as the RTV concentration increased, the K_m increased, but the k_{cat} decreased. Therefore, the K_i value (0.33 μM RTV) was obtained by fitting the data using nonlinear regression for mixed-

DMD Fast Forward. Published on July 25, 2013 as DOI: 10.1124/dmd.113.053108
This article has not been copyedited and formatted. The final version may differ from this version.

type inhibition as described in Materials and Methods. To be able to visualize the inhibition better, a Dixon plot of $1/k_{cat}$ versus the RTV concentrations is presented to show mixed type inhibition with a K_i value of ~0.3 μM for the RTV (Fig. 5B). The K_i values obtained from the two methods are in relatively good agreement.

Difference Spectrum for the Binding of RTV to CYP2B6. The binding of RTV to CYP2B6 induced a change in the absolute spectrum with an increase in the maximum wavelength of absorption of ~5 nm (Fig. 6A). The difference absorbance spectra for the addition of increasing concentrations of RTV are displayed in Fig. 6B. These results with a peak at ~428 nm and a trough at ~405 nm indicate that RTV is a type II ligand for CYP2B6. The K_s for the binding of RTV to CYP2B6 was determined to be 0.85 μM by fitting the data from Fig. 6B to the Michalis-Menten equation (inset) as described in Materials and Methods.

Modification of the Prosthetic Heme during Inactivation of CYP2B6 by RTV. The reaction mixtures incubated with 10 μM RTV in the absence (control) or presence (inactivated) of NADPH for 10 min were analyzed by HPLC to determine the extent and nature of heme modification. The column eluates were monitored at 400 nm. As shown in Fig. 7A, there was ~50% decrease in the prosthetic heme following the inactivation of CYP2B6, but no heme adduct could be observed.

Investigation of the CYP2B6 Apoprotein Modification by RTV. Using the same conditions for inactivation as were used for heme analysis, the mass of the apoprotein

before and after inactivation was determined by ESI-LC-MS analysis. As shown in Fig. 7B, the control CYP2B6 apoprotein exhibited a mass of 54453 ± 10 Da and the RTV-inactivated CYP2B6 apoprotein exhibited a mass of 54451 ± 8 Da without showing an additional peak that would have been expected as a result of the formation of a protein adduct. These results suggest that significant covalent modification of the apoprotein by a reactive intermediate did not occur. Under these conditions, the catalytic activity of the inactivated sample decreased ~50%, suggesting that the loss of catalytic activity was due primarily to the heme modification.

Heme Modification Following RTV-Inactivation in CYP3A4. Although RTV has previously been shown to be a potent mechanism-based inactivator of CYP3A4, the ability of RTV to act as a mechanism-based inactivator in a CYP3A4 reconstituted system was investigated as described under *Materials and Methods*. In agreement with previous reports, the kinetic values of K_I and k_{inact} were determined to be 0.05 μM and 0.1 min^{-1}, respectively, indicating that RTV is a potent mechanism-based inactivator of CYP3A4 in a reconstituted system used in our laboratory (data not shown). Using the same procedure as described for CYP2B6, CYP3A4 was incubated with 2 μM RTV for 10 min in the absence or presence of NADPH and then analyzed by HPLC. A ~50% decrease in prosthetic heme eluting at 26.0 min was observed in the RTV-inactivated CYP3A4 with the formation of a heme adduct eluting at ~31.5 min but not in the control sample (Fig. 8A). Magnified views of the control and inactivated samples are also displayed to better show the peaks for the heme-protein adduct. Figure 8B shows the chromatogram of the sample monitored at 220 nm showing that CYP3A4 also elutes at

31.5 min. Furthermore, analysis of the two peaks using a photodiode-array detector coupled to the HPLC shows that the wavelength for the maximal absorbance of the native heme eluting at 26.0 min is ~398 nm, whereas the peak eluting at 31.5 min exhibits maximal absorbance at ~278 nm (apoprotein) and ~397 nm (heme) (Fig. 8C). The peak at 31.5 min could be due to formation of a covalent bond between the prosthetic heme and the apoprotein or to the presence of a dissociable modified RTV-heme adduct that coelutes with the apoproten. In most the cases, the maximal absorption spectrum of a dissociable heme adduct is red-shifted by 5 to 10 nm, whereas the maximal absorption spectrum of the native heme is ~398 nm (Lin and Hollenberg, 2007; Lin et al, 2009). The same retention time for the heme adduct and the apoprotein and the evidence of two maximal absorbances of this peak at ~278 nm and ~397 nm suggests that this peak probably is due to cross-linking of the prosthetic heme moiety to the apoprotein during the mechanism-based inactivation of CYP3A4 by RTV. Similar types of crosslinking have previously been reported by Osawa and Pohl (Osawa and Pohl, 1989). Similar to CYP2B6, modification of the apoprotein by RTV was not observed for the inactivated CYP3A4 (data not shown).

LC-MS/MS Analysis of the RTV-GSH Conjugate Formed by CYP3A4 and Human Liver Microsomes. In order to identify the reactive intermediate formed during the metabolism of RTV by CYP2B6, CYP3A4, and human liver microsomes, incubations were performed in the presence of 10 mM GSH and the RTV-GSH conjugates were characterized by LC-MS/MS analysis as described in Materials and Methods. The extracted ion chromatogram for the GSH conjugate with a precursor ion at *m/z* 858 shows

a single peak eluting at 28.9 min for the RTV-inactivated CYP3A4 sample (Fig. 9A). The MS/MS spectrum of this RTV-GSH conjugate is displayed in Fig. 9B. The major fragment ion at *m/z* 840 is from the loss of water, the fragment ion at *m/z* 783 is from the loss of Gly (75 Da), the fragment ion at *m/z* 729 is from loss of Glu (129 Da) and further loss of water leads to formation of the ion at *m/z* 711. All of these fragment ions indicate that GSH is a component of the RTV-GSH conjugate (Baillie and Davis, 1993). It is worth noting that the fragment ions of the RTV-GSH conjugate at *m/z* 551, 525, 507, 426, and 311 are also observed in the MS/MS spectra of metabolite b (MH^+ ion at *m/z* 582) as shown in Fig. 2. These results facilitate the identification of the chemical structure for the reactive intermediate. The molecular mass of the GSH conjugate is equivalent to the sum of GSH plus the proposed reactive metabolite intermediate, thus the mass of the reactive intermediate would be 550 Da (858 Da minus 308 Da). Moreover, previous studies have demonstrated that *p*-chlorophenyl isocyanate forms a conjugate with GSH (Jochheim et al., 2002; Chen et al., 2009). Therefore, we hypothesize that the reactive metabolite is an isocyanate intermediate formed by the loss of the "HN-CH_3" moiety from metabolite b. However, the chemical mechanism for the formation of the isocyanate intermediate is not clear and other possibilities for the formation of reactive intermediates trapped by GSH cannot be excluded. It will be interest to further investigate other possibilities including an imine or a hydroxamic acid as the reactive intermediate. The proposed structure for the RTV-GSH conjugate eluting at 28.9 min is shown in Fig. 9C. The sites for the MS/MS fragmentation are indicated by the dashed lines. The RTV-GSH conjugate formed by human liver microsomes incubated with RTV and NADPH is essentially the same as this (data not shown). However, the formation of a RTV-GSH

conjugate by CYP2B6 was not sufficient for the accurate MS/MS spectrum analysis (data not shown).

Identification of a Stable Metabolite formed from the Isocyanate Intermediate of RTV formed by CYP3A4 and Human Liver Microsomes. To investigate the possibility that an isocyanate intermediate formed during the metabolism of RTV by CYP3A4 and human liver microsomes can lead to the formation of the RTV-GSH conjugate, the formation of a possible stable metabolite was investigated. The stable amine metabolite, which can be formed from hydrolysis followed by loss of CO_2 from the isocyanate intermediate, has been shown to be formed from isocyanate intermediates such as *p*-chlorophenyl isocyanate (Jochheim et al., 2002; Chen et al., 2009). The mass of the stable amine metabolite is expected to be 26 Da (+ H_2O – CO_2) less than the isocyanate intermediate, thus the molecular ion would be at *m/z* 525 Da. The extracted ion chromatogram at *m/z* 525 shows one major metabolite, which eluted at 31.8 min as shown in Fig. 10A. The MS/MS spectrum of the ion at *m/z* 525 is shown in Fig. 10B. Several fragment ions in this MS/MS spectrum are in common with the precursor ions for the metabolite with *m/z* 858 and *m/z* 525 such as the ions at *m/z* 311, 410, 426, 481, and 507. Figure 10C shows the structure proposed for the stable amine metabolite with a MH^+ ion at *m/z* 525 and the sites of fragmentation are indicated by the dashed lines.

Discussion

RTV is an important and widely used PI for anti-HIV therapy. RTV is a potent inhibitor and a mechanism-based inactivator of CYP3A4; therefore, it is used at low doses (100-300 mg) in combination with other PIs to boost their bioavailability and therapeutic effect (Foisy et al., 2008; Hull and Montaner, 2011; Kirby et al., 2011a; Kirby et al., 2011b). The crystal structures of the CYP3A4-RTV complex and a CYP3A4-RTV analog complex have recently been reported. These studies provided the first functional and structural insights into the interaction of RTV with CYP3A4 and demonstrated the relative importance of heme coordination and non-bonded interactions (Sevrioukova and Poulous 2010; Sevrioukova and Poulous 2012). The interactions of RTV with CYP3A4 at the *in vivo* levels are complex and involve multiple modes of interaction including inhibition, inactivation and induction (Kirby et al., 2011b). To complicate the interaction potential even further, RTV induces expression of other drug metabolizing P450s including 1A2, 2B6, and 2C9 (Kharasch et al., 2008; Kirby et al., 2011a). Additional studies in an animal model have demonstrated that the toxicity of RTV may be due to its bioactivation (Li et al., 2011). Since the inhibition and induction of CYP2B6 by RTV has been demonstrated, we investigated the metabolism of RTV by CYP2B6 and the ability of RTV to act as a mechanism-based inactivator.

Two major metabolites are generated as result of metabolism of RTV by CYP2B6. The first is formed through deacylation of RTV (metabolite a) and the second results from hydroxylation of the isopropyl-thiazole group (metabolite c). These two metabolites were identified by comparing the retention times and MS/MS spectra to the four major metabolites formed by CYP3A4 (Kumar et al., 1996; Koudriakova et al.,

DMD Fast Forward. Published on July 25, 2013 as DOI: 10.1124/dmd.113.053108
This article has not been copyedited and formatted. The final version may differ from this version.

1998). At this time, RTV appears to be the largest compound that can be metabolized by CYP2B6.

The apparent K_I and k_{inact} values for inactivation by RTV are 0.9 μM and 0.05 min^{-1}, respectively, and the partition ratio is ~3. These results indicate that RTV is an efficient mechanism-based inactivator of CYP2B6. In addition, RTV is a mixed type inhibitor of CYP2B6. The K_i was determined to be at ~0.3 μM RTV. The inhibitory potency is the same order of magnitude as three relatively potent and selective inhibitors of CYP2B6: 4-benzylpyridine, 4-(4-chlorobenzyl)pyridine and 4-(4-nitrobenyl)pyridine (Korhonen et al., 2007) and four clinically important drugs: clopidogrel, clotrimazole, sertraline and ticlopidine (Talakad et al., 2009). RTV produced a type II difference spectrum with the K_s of 0.85 μM. Previously, RTV has been characterized as a type II ligand for CYP3A4 and the thiazole nitrogen was proposed to be critical for ligation to the heme iron (Kempf et al., 1997; Servriouklova aand Poulos, 2010). Whether RTV binding to CYP2B6 involves the same ligation of the thiazole nitrogen to the heme iron as in CYP3A4 is not clear.

In spite of the widespread use of RTV in anti-HIV therapy and the numerous studies of its metabolism in vivo and in vitro, the molecular mechanism by which RTV is a mechanism-based inactivator of CYP3A4 has not been determined (Koudriakova et al., 1998; Ernest et al., 2005; Sevrioukova and Poulos, 2010). Here, HPLC and LC-MS analysis revealed that inactivation is due to heme destruction and there is no significant modification of the apoprotein during RTV-mediated inactivation of either CYP2B6 or CYP3A4. The reconstituted systems used for these studies contained only P450 and CPR

without the addition of cytochrome b_5. Because the heme moieties of P450 and cytochrome b_5 coelute during HPLC analysis, cytochrome b_5 was not added to the reconstituted systems in order to avoid interference from the heme moiety of cytochrome b_5 (Lin et al., 2002). Therefore, we can conclude that the predominant mechanism contributing to the mechanism-based inactivation for both CYP3A4 and CYP2B6 is heme destruction.

The formation of a heme-protein adduct was observed during the mechanism-based inactivation of CYP3A4 by RTV. Although the conversion to the heme adduct does not appear to be quantitative with respect to heme loss, it is possible that more adduct may have been formed initially but, it was not stable during the HPLC analysis under acidic conditions. We have proposed that the heme adduct formed during the mechanism-based inactivation of CYP3A4 by RTV forms a covalent cross-link with the apoprotein. Osawa and Pohl (1989) have proposed two mechanisms for the covalent binding of heme to apoprotein. The first pathway involves reaction of a substrate radical with the heme prosthetic group to form an activated cation heme intermediate, which could then covalently bind to the side chain a polar amino acid in the protein active site. In this case, the reactive intermediate formed from RTV would be attached as part of the heme-protein adduct. The second possible pathway leading to the formation of protein bound heme adduct involves the initial attack of the reactive substrate radical on the protein to form an amino acid radical which can then react to form a covalent adduct with the heme moiety. In this case, there would be no reactive intermediate of RTV attached to the heme-protein adduct. Because we were not able to obtain sufficient quantities of the

heme-protein adduct of CYP3A4 formed during the inactivation to analyze the modified protein by mass spectrometry, we have not been able to ascertain which mechanism is contributing to the formation of the heme-protein adduct. This is the first report of the formation of a heme-protein adduct during the inactivation of any human P450 by RTV.

It has been suggested that the presence of both the thiazole and the isopropyl-thiazole group as well as the formation of a reactive intermediate during metabolism are required for RTV to inactivate of CYP3A4 (Kempf et al., 1997; Koudriakova et al., 1998; Sevrioukova and Poulos, 2010). By trapping the reactive intermediates of mechanism-based inactivators of P450s as their GSH conjugates, we have previously been able to identify the reactive intermediates responsible for mechanism-based inactivation of P450s by a number of compounds including 17α-ethynylestradiol, bergamottin, mifepristone, and *tert*-butylphenylacetylene (Kent et al., 2006; Lin et al., 2009; Lin et al., 2011; Lin et al., 2012). Using our previous experimental procedures, an RTV-GSH conjugate with its MH^+ ion at *m/z* 858 was identified following incubation of RTV with both CYP3A4 and human liver microsomes in the presence NADPH and GSH. Based on the fragmentation patterns observed on LC-MS/MS analysis and the identification of a stable amine metabolite with its MH^+ ion at *m/z* 525, we propose that the reactive intermediate formed following bioactivation of RTV is an isocyanate. The pathway for the formation of isocyanate from RTV, the further formation of a GSH conjugate, and the formation of the stable amine metabolite after hydrolysis and loss of CO_2 are shown in Fig. 11. This is the first report of trapping of a reactive metabolite of RTV and the formation of a stable amine metabolite during RTV metabolism by a human P450 as well as by human liver microsomes. In addition to reacting with GSH or undergoing

hydrolysis, isocyanate intermediates can also carbamoylate proteins; thus, isocyanates formed by hydrolysis of isothiocyanates have been implicated as being the reactive species leading to mechanism-based inactivation of human and rat P450s (Goosen et al., 2001; Moreno et al., 2001). Because neither a dissociable heme adduct nor an apoprotein adduct could be identified, the mass of the reactive intermediate contributing to the mechanism-based inactivation of CYP2B6 and CYP3A4 by RTV cannot be elucidated. However, isocyanates have been implicated to play roles in the hypersensitivity of the skin and respiratory tract and have the potential to result in toxicity (Goossens et al., 2002; Jochheim et al., 2002; Liu and Wisnewski, 2003). It has been reported that adverse effects including hepataotoxicity and skin hypersensitivity have been observed following treatment of HIV-patients with RTV (Floridia et al., 2004; Bruno et al., 2006). We have proposed here the formation of an isocyanate intermediate during the metabolism of RTV by human liver microsomes. Perhaps, this isocyanate intermediate may play a critical role in the adverse effects associated with RTV treatment.

In conclusion, RTV is a mechanism-based inactivator of CYP2B6. It is the largest clinically used drug (MW = 721 Da) metabolized by CYP2B6 that has been identified thus far. The primary mechanism responsible for the mechanism-based inactivation of both CYP2B6 and CYP3A4 is heme destruction. In addition, formation of a protein-bound heme adduct was observed following inactivation of CYP3A4 by RTV. Since depression, cardiovascular diseases and other complications frequently accompany HIV infection (Ferrando et al., 1997; Avants et al., 1998; Greenblatt et al., 1999; Hesse et al., 2001; Daali et al., 2011), it is likely that HIV patients may take drugs preferentially metabolized by CYP2B6 including bupropion, prasugrel, or methadone. Therefore,

during the treatment of HIV patients with RTV, concomitant use drugs metabolized solely or primarily by CYP2B6 may require dosage adjustment to prevent toxicity.

Acknowledgments

We thank Dr. R. Neubig, Department of Pharmacology, University of Michigan (Ann Arbor, MI) for the use of the Wallace Victor II counter.

Authorship Contribution

Participated in research design: Lin, Kenaan, and D'Agostino.

Conducted experiments: Lin and D'Agostino.

Contributed new reagents or analytical tools: Lin, Kenaan, and D'Agostino.

Performed data analysis: Lin, D'Agostino, and Kenaan.

Wrote or contributed to writing of manuscript: Lin, Calinski, D'Agostino, Kenaan, and Hollenberg.

References

Avants SK, Margolin A, DePhilippis D, and Kosten TR (1998) A comprehensive pharmacologic-psychosocial treatment program for HIV-seropositive cocaine- and opioid-dependent patients. Preliminary findings. *J Subst Abuse Treat* **15:**261-265.

Baillie TA and Davis MR (1993) Mass spectrometry in the analysis of glutathione conjugates. *Biol Mass Spectrom* **22:**319-325.

Bruno R, Sacchi P, Maiocchi L, Patruno S, and Filice G (2006) Hepatotoxicity and antiretroviral therapy with protease inhibitors: A review. *Dig Liver Dis* **38:**363-373.

Chen H, Zientek M, Jalaie M, Zhang Y, Bigge C, and Mutlib A (2009) Characterization of cytochrome P450-mediated bioactivation of a compound containing the chemical scaffold, 4,5-dihydropyrazole-1-carboxylic acid-(4-chlorophenyl amide), to a chemically reactive p-chlorophenyl isocyanate intermediate in human liver microsomes. *Chem Res Toxicol* **22:**1603-1612.

Daali Y, Ancrenaz V, Bosilkovska M, Dayer P, and Desmeules J (2011) Ritonavir inhibits the two main prasugrel bioactivation pathways in vitro: a potential drug-drug interaction in HIV patients. *Metabolism* **60:**1584-1589.

Duggan ST and Keating GM (2009) Prasugrel: a review of its use in patients with acute coronary syndromes undergoing percutaneous coronary intervention. *Drugs* **69:**1707-1726.

Ernest CS, 2nd, Hall SD, and Jones DR (2005) Mechanism-based inactivation of CYP3A by HIV protease inhibitors. *J Pharmacol Exp Ther* **312:**583-591.

Ferrando SJ, Goldman JD, and Charness WE (1997) Selective serotonin reuptake inhibitor treatment of depression in symptomatic HIV infection and AIDS. Improvements in affective and somatic symptoms. *Gen Hosp Psychiatry* **19:**89-97.

Floridia M, Bucciardini R, Fragola V, Galluzzo CM, Giannini G, Pirillo MF, Amici R, Andreotti M, Ricciardulli D, Tomino C, and Vella S (2004) Risk factors and occurrence of rash in HIV-positive patients not receiving nonnucleoside reverse transcriptase inhibitor: data from a randomized study evaluating use of protease inhibitors in nucleoside-experienced patients with very low CD4 levels (<50 cells/microL). *HIV Med* **5:**1-10.

Foisy MM, Yakiwchuk EM, and Hughes CA (2008) Induction effects of ritonavir: implications for drug interactions. *Ann Pharmacother* **42:**1048-1059.

Gervot L, Rochat B, Gautier JC, Bohnenstengel F, Kroemer H, de Berardinis V, Martin H, Beaune P, and de Waziers I (1999) Human CYP2B6: expression, inducibility and catalytic activities. *Pharmacogenetics* **9:**295-306.

Goosen TC, Mills DE, and Hollenberg PF (2001) Effects of benzyl isothiocyanate on rat and human cytochromes P450: identification of metabolites formed by P450 2B1. *J Pharmacol Exp Ther* **296:**198-206.

Goossens A, Detienne T, and Bruze M (2002) Occupational allergic contact dermatitis caused by isocyanates. *Contact Dermatitis* **47:**304-308.

Granfors MT, Wang JS, Kajosaari LI, Laitila J, Neuvonen PJ, and Backman JT (2006) Differential inhibition of cytochrome P450 3A4, 3A5 and 3A7 by five human immunodeficiency virus (HIV) protease inhibitors in vitro. *Basic Clin Pharmacol Toxicol* **98:**79-85.

Greenblatt DJ, von Moltke LL, Daily JP, Harmatz JS, and Shader RI (1999) Extensive impairment of triazolam and alprazolam clearance by short-term low-dose ritonavir: the clinical dilemma of concurrent inhibition and induction. *J Clin Psychopharmacol* **19:**293-296.

Hesse LM, von Moltke LL, Shader RI, and Greenblatt DJ (2001) Ritonavir, efavirenz, and nelfinavir inhibit CYP2B6 activity in vitro: potential drug interactions with bupropion. *Drug Metab Dispos* **29:**100-102.

Hull MW and Montaner JS (2011) Ritonavir-boosted protease inhibitors in HIV therapy. *Ann Med* **43:**375-388.

Jochheim CM, Davis MR, Baillie KM, Ehlhardt WJ, and Baillie TA (2002) Glutathione-dependent metabolism of the antitumor agent sulofenur. Evidence for the formation of p-chlorophenyl isocyanate as a reactive intermediate. *Chem Res Toxicol* **15:**240-248.

Kempf DJ, Marsh KC, Kumar G, Rodrigues AD, Denissen JF, McDonald E, Kukulka MJ, Hsu A, Granneman GR, Baroldi PA, Sun E, Pizzuti D, Plattner JJ, Norbeck DW, and Leonard JM (1997) Pharmacokinetic enhancement of inhibitors of the human immunodeficiency virus protease by coadministration with ritonavir. *Antimicrob Agents Chemother* **41:**654-660.

Kent UM, Lin HL, Mills DE, Regal KA, and Hollenberg PF (2006) Identification of 17-alpha-ethynylestradiol-modified active site peptides and glutathione conjugates formed during metabolism and inactivation of P450s 2B1 and 2B6. *Chem Res Toxicol* **19:**279-287.

Kharasch ED, Mitchell D, Coles R, and Blanco R (2008) Rapid clinical induction of hepatic cytochrome P4502B6 activity by ritonavir. *Antimicrob Agents Chemother* **52:**1663-1669.

Kirby BJ, Collier AC, Kharasch ED, Dixit V, Desai P, Whittington D, Thummel KE, and Unadkat JD (2011a) Complex drug interactions of HIV protease inhibitors 2: in vivo induction and in vitro to in vivo correlation of induction of cytochrome P450 1A2, 2B6, and 2C9 by ritonavir or nelfinavir. *Drug Metab Dispos* **39:**2329-2337.

Kirby BJ, Collier AC, Kharasch ED, Whittington D, Thummel KE, and Unadkat JD (2011b) Complex drug interactions of HIV protease inhibitors 1: inactivation, induction, and inhibition of cytochrome P450 3A by ritonavir or nelfinavir. *Drug Metab Dispos* **39:**1070-1078.

Korhonen LE, Turpeinen M, Rahnasto M, Wittekindt C, Poso A, Pelkonen O, Raunio H, and Juvonen RO (2007) New potent and selective cytochrome P450 2B6 (CYP2B6) inhibitors based on three-dimensional quantitative structure-activity relationship (3D-QSAR) analysis. *Br J Pharmacol* **150:**932-942.

Koudriakova T, Iatsimirskaia E, Utkin I, Gangl E, Vouros P, Storozhuk E, Orza D, Marinina J, and Gerber N (1998) Metabolism of the human immunodeficiency virus protease inhibitors indinavir and ritonavir by human intestinal microsomes

and expressed cytochrome P4503A4/3A5: mechanism-based inactivation of cytochrome P4503A by ritonavir. *Drug Metab Dispos* **26:**552-561.

Kumar GN, Rodrigues AD, Buko AM, and Denissen JF (1996) Cytochrome P450-mediated metabolism of the HIV-1 protease inhibitor ritonavir (ABT-538) in human liver microsomes. *J Pharmacol Exp Ther* **277:**423-431.

Lang T, Klein K, Fischer J, Nussler AK, Neuhaus P, Hofmann U, Eichelbaum M, Schwab M, and Zanger UM (2001) Extensive genetic polymorphism in the human CYP2B6 gene with impact on expression and function in human liver. *Pharmacogenetics* **11:**399-415.

Li F, Lu J, and Ma X (2011) Metabolomic screening and identification of the bioactivation pathways of ritonavir. *Chem Res Toxicol* **24:**2109-2114.

Lin HL and Hollenberg PF (2007) The inactivation of cytochrome P450 3A5 by 17alpha-ethynylestradiol is cytochrome b5-dependent: metabolic activation of the ethynyl moiety leads to the formation of glutathione conjugates, a heme adduct, and covalent binding to the apoprotein. *J Pharmacol Exp Ther* **321:**276-287.

Lin HL, Kenaan C, and Hollenberg PF (2012) Identification of the residue in human CYP3A4 that is covalently modified by bergamottin and the reactive intermediate that contributes to the grapefruit juice effect. *Drug Metab Dispos* **40:**998-1006.

Lin HL, Kent UM, and Hollenberg PF (2002) Mechanism-based inactivation of cytochrome P450 3A4 by 17 alpha-ethynylestradiol: evidence for heme destruction and covalent binding to protein. *J Pharmacol Exp Ther* **301:**160-167.

Lin HL, Zhang H, and Hollenberg PF (2009) Metabolic activation of mifepristone [RU486; 17beta-hydroxy-11beta-(4-dimethylaminophenyl)-17alpha-(1-propynyl)-

estra-4,9-dien -3-one] by mammalian cytochromes P450 and the mechanism-based inactivation of human CYP2B6. *J Pharmacol Exp Ther* **329:**26-37.

Lin HL, Zhang H, Pratt-Hyatt MJ, and Hollenberg PF (2011) Thr302 is the site for the covalent modification of human cytochrome P450 2B6 leading to mechanism-based inactivation by tert-butylphenylacetylene. *Drug Metab Dispos* **39:**2431-2439.

Liu Q and Wisnewski AV (2003) Recent developments in diisocyanate asthma. *Ann Allergy Asthma Immunol* **90:**35-41.

Moreno RL, Goosen T, Kent UM, Chung FL, and Hollenberg PF (2001) Differential effects of naturally occurring isothiocyanates on the activities of cytochrome P450 2E1 and the mutant P450 2E1 T303A. *Arch Biochem Biophys* **391:**99-110.

Osawa Y and Pohl LR (1989) Covalent bonding of the prosthetic heme to protein: a potential mechanism for the suicide inactivation or activation of hemoproteins. *Chem Res Toxicol* **2:**131-141.

Palella FJ, Jr., Delaney KM, Moorman AC, Loveless MO, Fuhrer J, Satten GA, Aschman DJ, and Holmberg SD (1998) Declining morbidity and mortality among patients with advanced human immunodeficiency virus infection. HIV Outpatient Study Investigators. *N Engl J Med* **338:**853-860.

Piscitelli SC, Flexner C, Minor JR, Polis MA, and Masur H (1996) Drug interactions in patients infected with human immunodeficiency virus. *Clin Infect Dis* **23:**685-693.

Sabin CA, Worm SW, Weber R, Reiss P, El-Sadr W, Dabis F, De Wit S, Law M, D'Arminio Monforte A, Friis-Moller N, Kirk O, Pradier C, Weller I, Phillips AN,

and Lundgren JD (2008) Use of nucleoside reverse transcriptase inhibitors and risk of myocardial infarction in HIV-infected patients enrolled in the D:A:D study: a multi-cohort collaboration. *Lancet* **371:**1417-1426.

Scott EE, Spatzenegger M, and Halpert JR (2001) A truncation of 2B subfamily cytochromes P450 yields increased expression levels, increased solubility, and decreased aggregation while retaining function. *Arch Biochem Biophys* **395:**57-68.

Sevrioukova IF and Poulos TL (2010) Structure and mechanism of the complex between cytochrome P4503A4 and ritonavir. *Proc Natl Acad Sci U S A* **107:**18422-18427.

Sevrioukova IF and Poulos TL (2012) Interaction of human cytochrome P4503A4 with ritonavir analogs. *Arch Biochem Biophys* **520:**108-116.

Silverman R (1996) Mechanism-Based Enzyme Inactivation, in Comtemporary Enzyme Kinetics and Mechanisms (Purich DL ed).pp 291-335 Academic Press, San Diego, CA.

Talakad JC, Kumar S, and Halpert JR (2009) Decreased susceptibility of the cytochrome P450 2B6 variant K262R to inhibition by several clinically important drugs. *Drug Metab Dispos* **37:**644-650.

Turpeinen M, Raunio H, and Pelkonen O (2006) The functional role of CYP2B6 in human drug metabolism: substrates and inhibitors in vitro, in vivo and in silico. *Curr Drug Metab* **7:**705-714.

von Moltke LL, Durol AL, Duan SX, and Greenblatt DJ (2000) Potent mechanism-based inhibition of human CYP3A in vitro by amprenavir and ritonavir: comparison with ketoconazole. *Eur J Clin Pharmacol* **56:**259-261.

von Moltke LL, Greenblatt DJ, Grassi JM, Granda BW, Duan SX, Fogelman SM, Daily JP, Harmatz JS, and Shader RI (1998) Protease inhibitors as inhibitors of human cytochromes P450: high risk associated with ritonavir. *J Clin Pharmacol* **38:**106-111.

Wang H and Tompkins LM (2008) CYP2B6: new insights into a historically overlooked cytochrome P450 isozyme. *Curr Drug Metab* **9:**598-610.

Zanger UM, Klein K, Saussele T, Blievernicht J, Hofmann MH, and Schwab M (2007) Polymorphic CYP2B6: molecular mechanisms and emerging clinical significance. *Pharmacogenomics* **8:**743-759.

Zeldin RK and Petruschke RA (2004) Pharmacological and therapeutic properties of ritonavir-boosted protease inhibitor therapy in HIV-infected patients. *J Antimicrob Chemother* **53:**4-9.

Zhang H, Lin HL, Walker VJ, Hamdane D, and Hollenberg PF (2009) tert-Butylphenylacetylene is a potent mechanism-based inactivator of cytochrome P450 2B4: inhibition of cytochrome P450 catalysis by steric hindrance. *Mol Pharmacol* **76:**1011-1018.

Footnote

This work was supported in part by National Institutes of Health Grant to PFH [CA-16954].

Legends for Figures

Fig. 1. LC-MS/MS analysis of the RTV metabolites formed by CYP3A4 and CYP2B6 in a reconstituted systems. Shown are the extracted ion chromatograms for RTV (ion at *m/z* 721), metabolite a (ion at *m/z* 580), metabolite b (ion at *m/z* 582), metabolite c (ion at *m/z* 737), and metabolite d (ion at *m/z* 707). CYP3A4 and CYP2B6 generated four and two major metabolites, respectively.

Fig. 2. Identification of four major metabolites of RTV. MS/MS spectra of RTV and the four major metabolites a, b, c and d. The spectra were obtained in positive mode using Xcalibur as described in Materials and Methods.

Fig. 3. Pathways proposed for the formation of four major metabolites of RTV. The chemical structures of RTV and the metabolites are displayed. The dashed lines indicate the sites of fragmentation, which give the fragment ions shown for each of metabolite in Fig. 2.

Fig. 4. Determination of the kinetic values and the partition ratio for CYP2B6 during inactivation by RTV. (A) The time- and concentration-dependent inactivation of CYP2B6 by RTV. The reconstituted system was incubated with 0 (●), 0.5 μM (■), 1 μM (▲), 3 μM (▽), 10 μM (◆), and 20 μM (○) RTV, aliquots were removed at the times indicated and assayed for residual EFC deethylation activity as described in *Materials and Methods* as shown in Fig. 3A. The catalytic activity at time zero was used as the

DMD Fast Forward. Published on July 25, 2013 as DOI: 10.1124/dmd.113.053108
This article has not been copyedited and formatted. The final version may differ from this version.

100% control to calculate the initial rate constants for the inactivation (k_{obs}) for each concentration of RTV. (B) Shows the fitting of the initial rate constants as a function of the RTV concentrations to the Michaelis-Menten equation. The K_I and k_{inact} values were determined to be 0.9 μM and 0.05 min^{-1}. (C) Determination of the partition ratio for 2B6 inactivation by RTV. The percentage of catalytic activity remaining was determined as a function of the molar ratio of RTV to CYP2B6 as described in *Materials and Methods*. The partition ratio was estimated from the intercept of the linear regression line from the lower ratios of RTV to 2B6 and the straight line obtained from the higher ratios of RTV to 2B6. The data represent the average of two separate experiments done in triplicate that did not differ by >10%.

Fig. 5. Studies on the reversible inhibition of CYP2B6-catalyzed EFC *O*-deethylation activity by RTV. (A) Determination the inhibition of CYP2B6 by RTV at varying concentreations of EFC. The RTV concentrations were 0 (●), 0.1 μM (□), 0.3 μM (▲), 0.6 μM (▽), and 1 μM (◆). The data presented were fitted to the Michaelis-Menten equation and the calculated kinetic parameters, K_m and K_{cat}, are shown in Table 1. The apparent K_i for RTV was determined to be 0.33 μM by nonlinear regression fitting to the equation for mixed type inhibition. (B) Dixon plot of the data in Fig. 4A, the concentrations of EFC are 1.0 μM (●), 2.5 μM (■), 5.0 μM (△), 10 μM (▼), 25μM (◇), and 50 μM (○). The apparent K_i (~0.3 μM RTV) was estimated from the intersection of the lines obtained at various concentrations of EFC.

Fig. 6. Spectra for RTV binding to CYP2B6. (A) Absolute spectra for CYP2B6 in the absence (solid line) or presence (dashed line) of 5 μM RTV. A shift of the maximal absorbance of 5 nm was observed. (B) RTV binding to CYP2B6 leading to a type II binding spectrum. The final concentrations of RTV added to the sample cuvette were: 0.3, 0.9, 2.4, 5.4, 10.4, 15.4, and 20 μM. Inset, the difference in the absorbance between the peak and the trough plotted versus the corresponding free RTV concentrations. The amount of RTV bound to 1 μM CYP2B6 at the lower concentrations was subtracted from the amount added, and the free concentrations of RTV used for the plot are 0.16, 0.5, 1.67, 5.4, 15.4, and 20 μM. The data points were fit to the Michaelis-Menten equation. The K_s was estimated to be 0.85 μM RTV.

Fig. 7. HPLC separation of CYP2B6 prosthetic heme group following inactivation by RTV. (A) HPLC elution profiles monitored at 400 nm for the prosthetic heme in the absence or presence of NADPH. (B) The deconvoluted mass spectra of CYP2B6 incubated with RTV in the absence or presence of NADPH. The experimental procedures are described under *Materials and Methods*.

Fig. 8. Modification of the heme prosthetic group of CYP3A4 following inactivation by RTV. (A) HPLC elution profiles monitored at 400 nm for prosthetic heme in the absence or presence of NADPH. Magnified views for the elution times from 24 to 34 min are displayed on the right showing formation of a heme-protein adduct eluting at 31.5 min in the inactivated sample. (B) HPLC profile of the reaction mixture monitored at 220 nm.

(C) Photodiode-array spectra of the native heme eluting at 26 min and the heme-protein adduct eluting at 31.5 min. The experimental procedures are described under *Materials and Methods*.

Fig. 9. LC-MS/MS analysis of the GSH conjugate formed during the metabolism of RTV. The reaction mixture containing CYP3A4 was incubated with RTV in the presence of NADPH and the reactive intermediate(s) were trapped with 10 mM GSH. The reaction mixture was analyzed for GSH conjugates as described under *Materials and Methods.* (A) The extracted ion chromatogram of the only GSH conjugate observed eluting at 28.9 min with the MH^+ ion at *m/z* 858. (B) The MS/MS spectrum of the GSH conjugate from A. (C) The proposed structure of the RTV-GSH conjugate based on the MS/MS spectrum. The dashed lines indicate the sites of fragmentation. The MS/MS spectrum was obtained in the positive mode and analyzed using the Xcalibur software package.

Fig. 10. LC-MS/MS analysis of the stable amine metabolite formed during the metabolism of RTV. (A) The extracted ion chromatogram of the stable amine metabolite eluting at 31.8 min with the MH^+ ion at *m/z* 525. B, The MS/MS spectrum of the metabolite. (C) Proposed structure of the stable amine metabolite. The dashed lines indicate the sites of fragmentation. The MS/MS spectra were obtained in the positive mode and analyzed using the Xcalibur software package.

Fig. 11. Scheme showing the P450-catalyzed bioactivation of RTV to the isocyanate intermediate and the reaction with GSH to form RTV-GSH conjugate or the further hydrolysis to stable amine metabolite (Jochheim et al., 2002; Chen et al., 2009).

DMD Fast Forward. Published on July 25, 2013 as DOI: 10.1124/dmd.113.053108
This article has not been copyedited and formatted. The final version may differ from this version.

Table 1. K_m and k_{cat} values for the CYP2B6-catalyzed deethylation of EFC in the presence of RTV[a].

RTV (μM)	K_m (μM)	k_{cat} (min^{-1})
0	1.83	0.80
0.1	2.05	0.67
0.3	2.47	0.54
0.6	2.68	0.44
1.0	4.00	0.37

[a]The concentrations of EFC used were: 1, 2.5, 5, 10, 25 and 50 μM.

Fig. 1

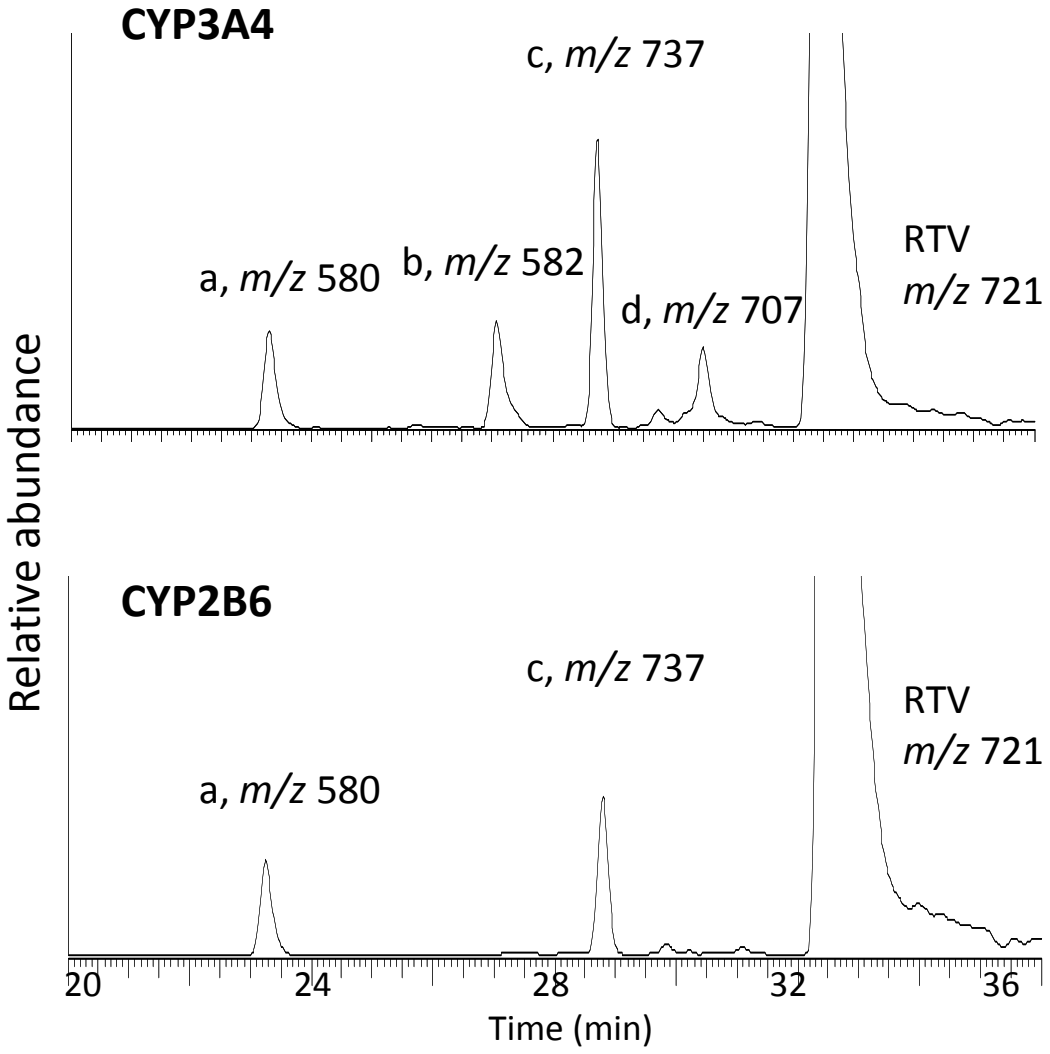
CYP3A4
c, m/z 737
a, m/z 580
b, m/z 582
d, m/z 707
RTV
m/z 721
CYP2B6
c, m/z 737
RTV
m/z 721
a, m/z 580
Relative abundance
20
24
28
32
36
Time (min)

Fig. 2

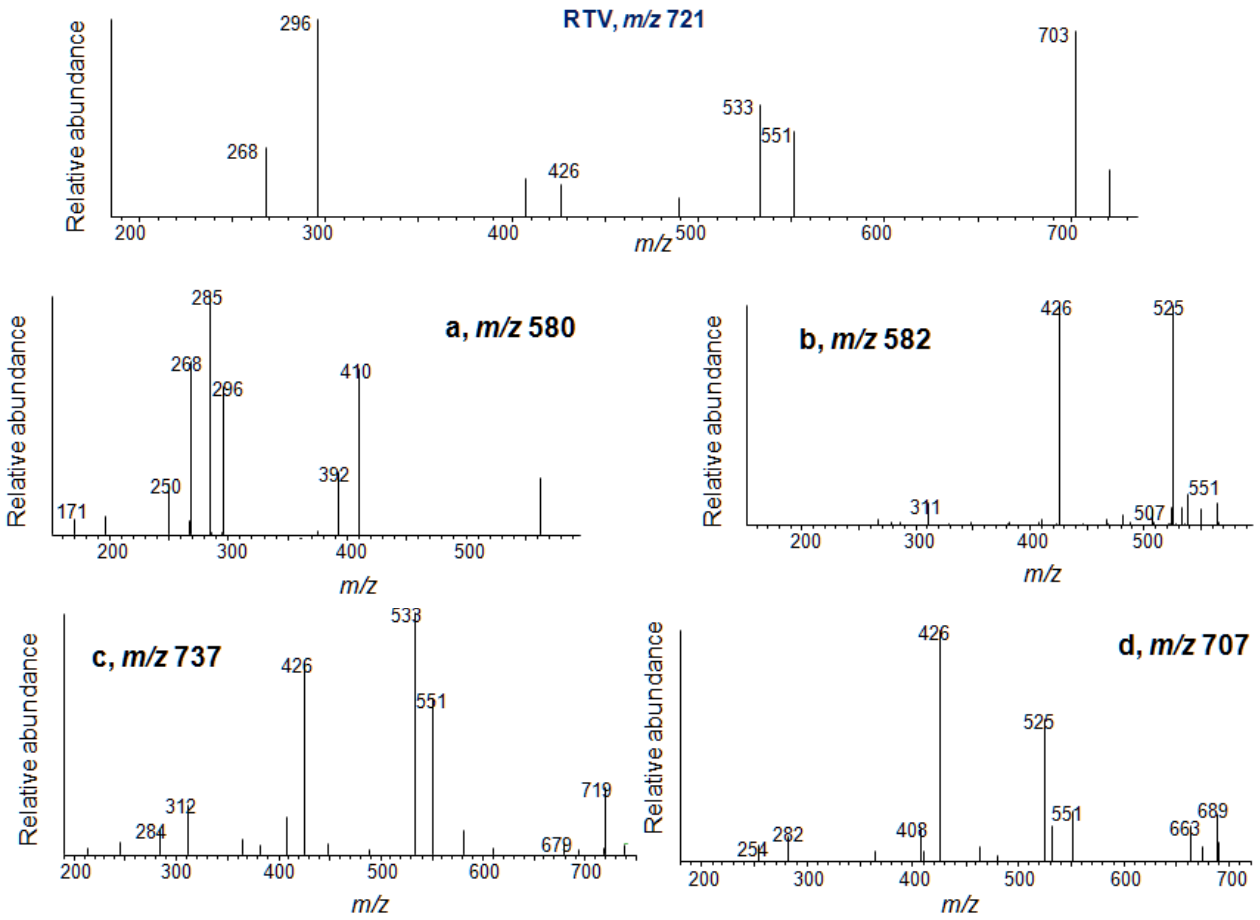

DMD Fast Forward. Published on July 25, 2013 as DOI: 10.1124/dmd.113.053108
This article has not been copyedited and formatted. The final version may differ from this version.

Fig. 3

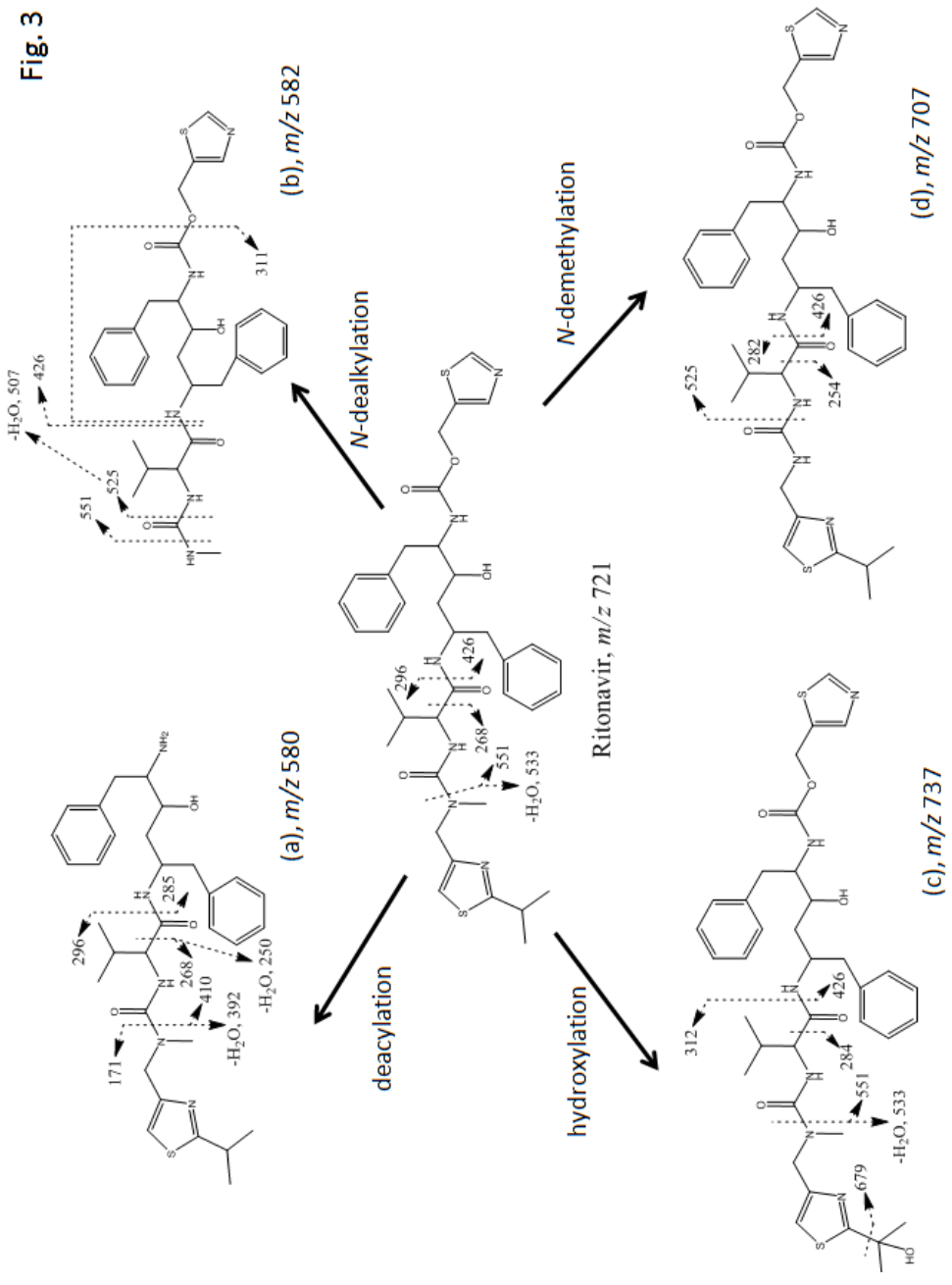

Fig. 4

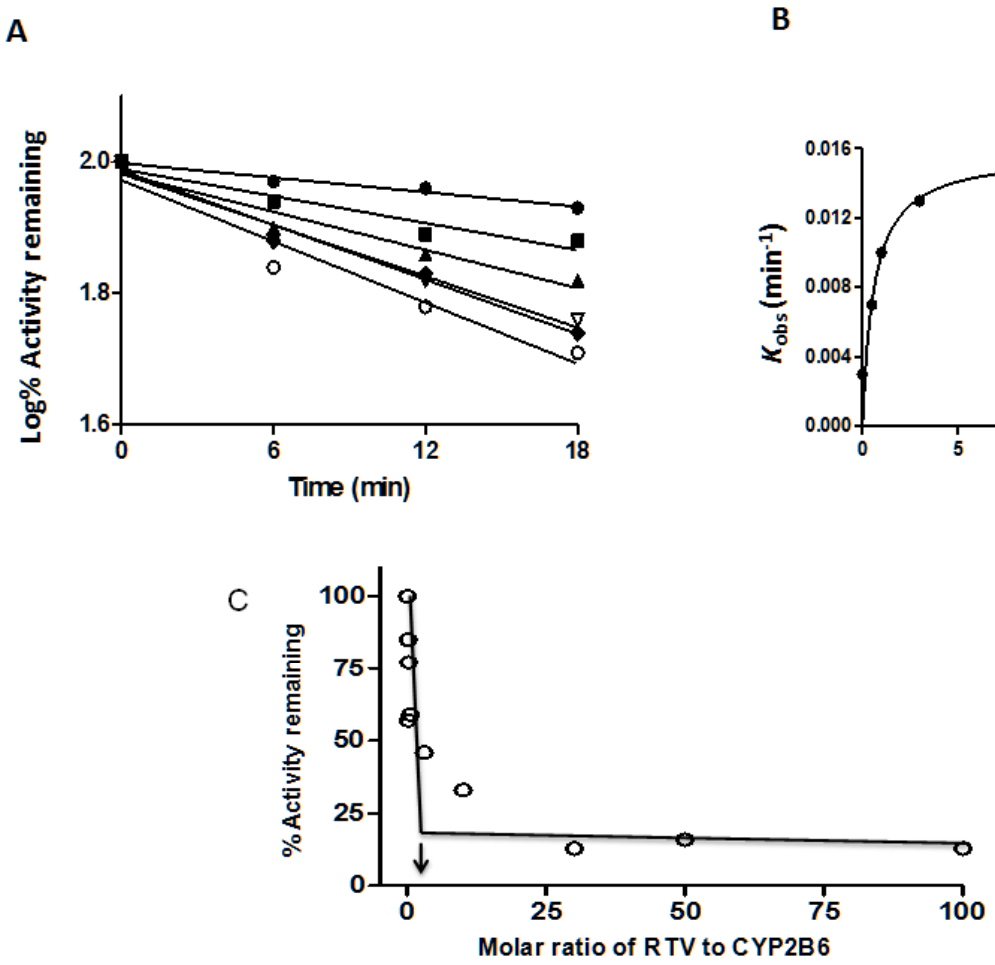

Fig. 5

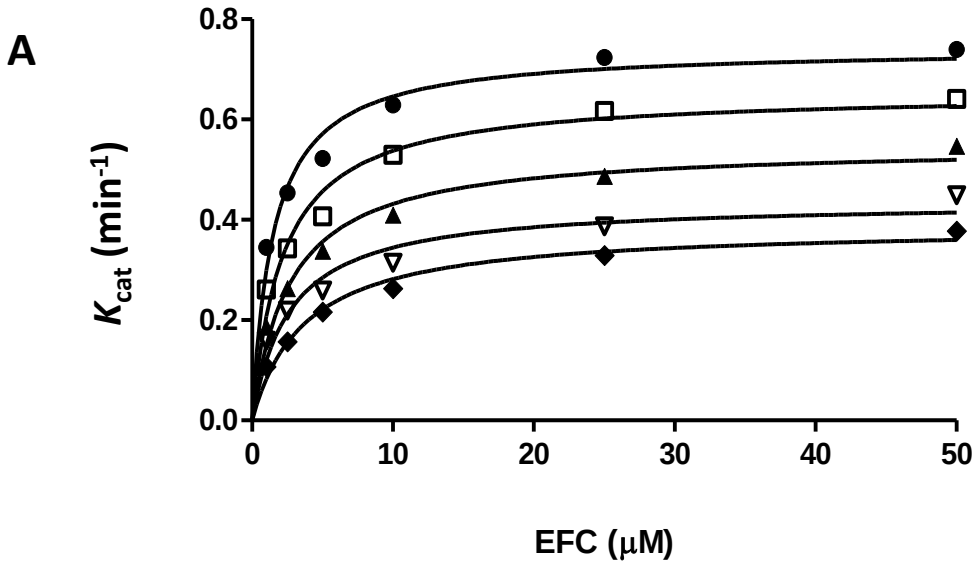

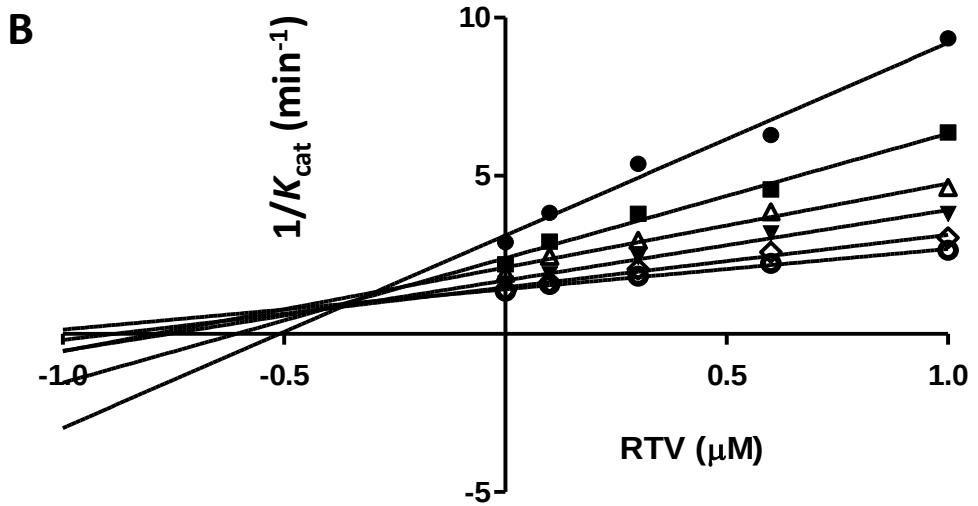

DMD Fast Forward. Published on July 25, 2013 as DOI: 10.1124/dmd.113.053108
This article has not been copyedited and formatted. The final version may differ from this version.

Fig. 6

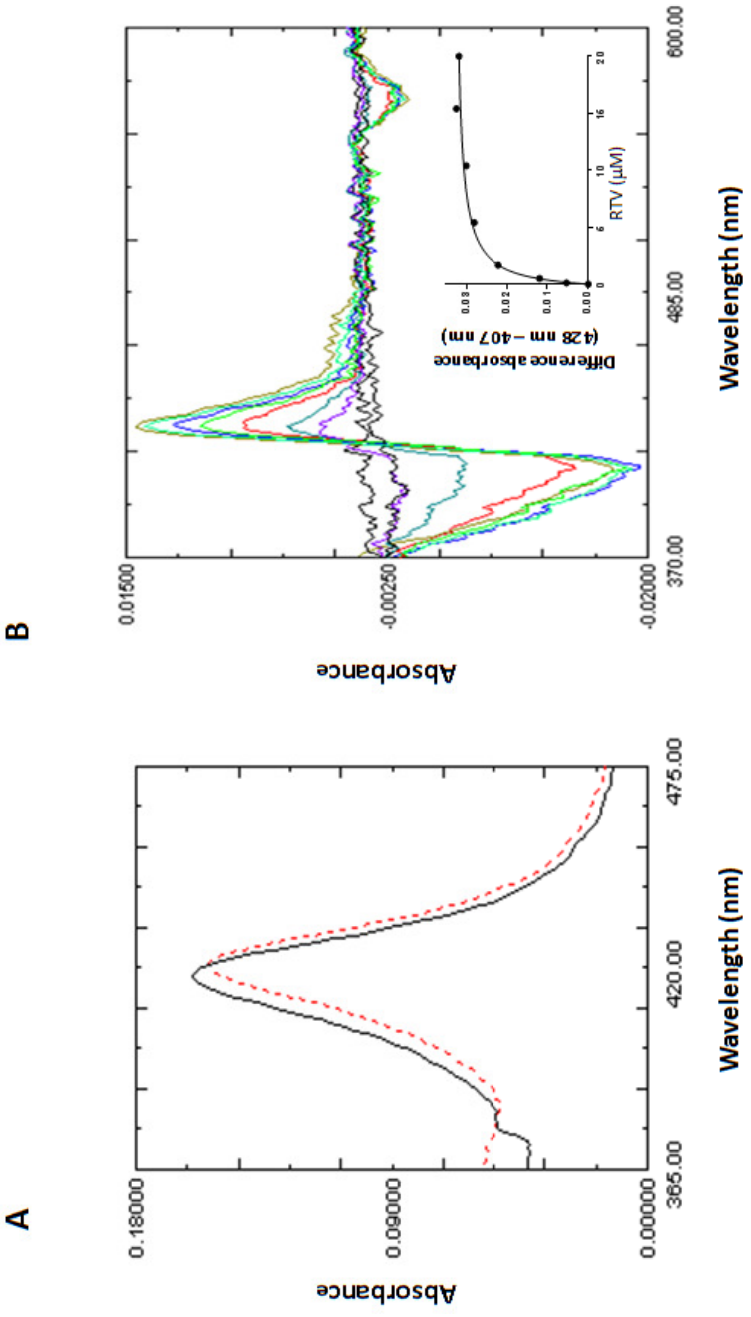

DMD Fast Forward. Published on July 25, 2013 as DOI: 10.1124/dmd.113.053108
This article has not been copyedited and formatted. The final version may differ from this version.

Fig. 7

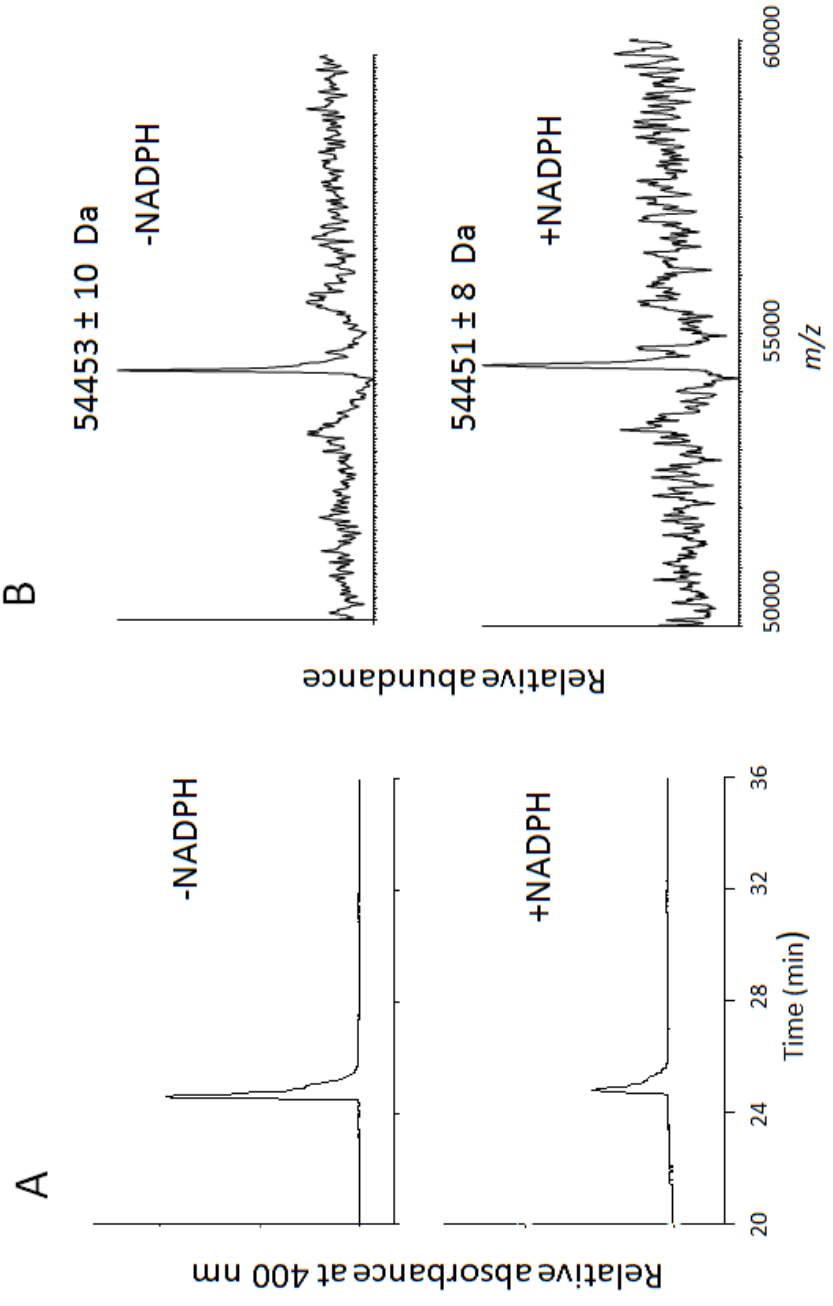

Fig. 8

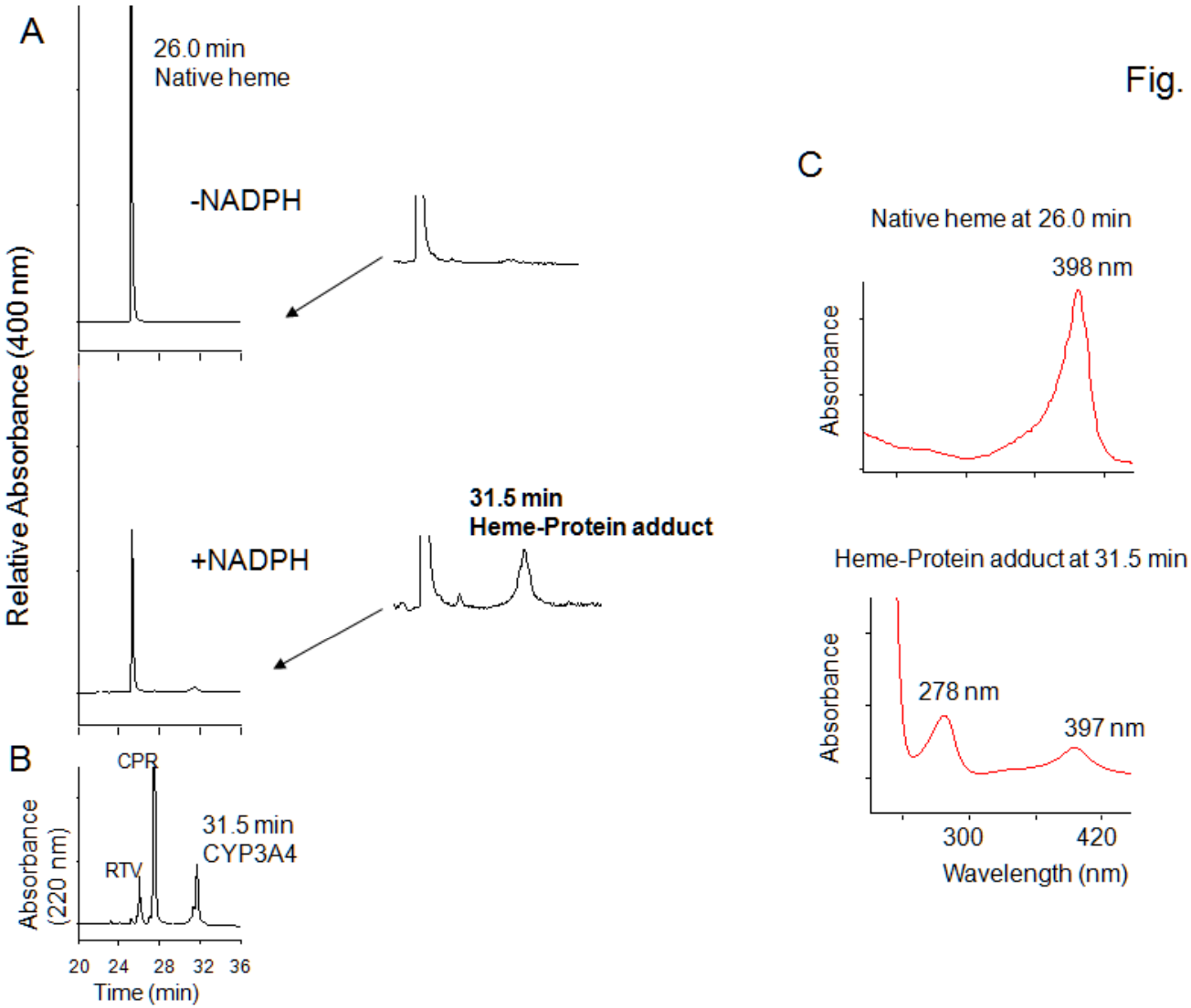

DMD Fast Forward. Published on July 25, 2013 as DOI: 10.1124/dmd.113.053108
This article has not been copyedited and formatted. The final version may differ from this version.

Fig. 9

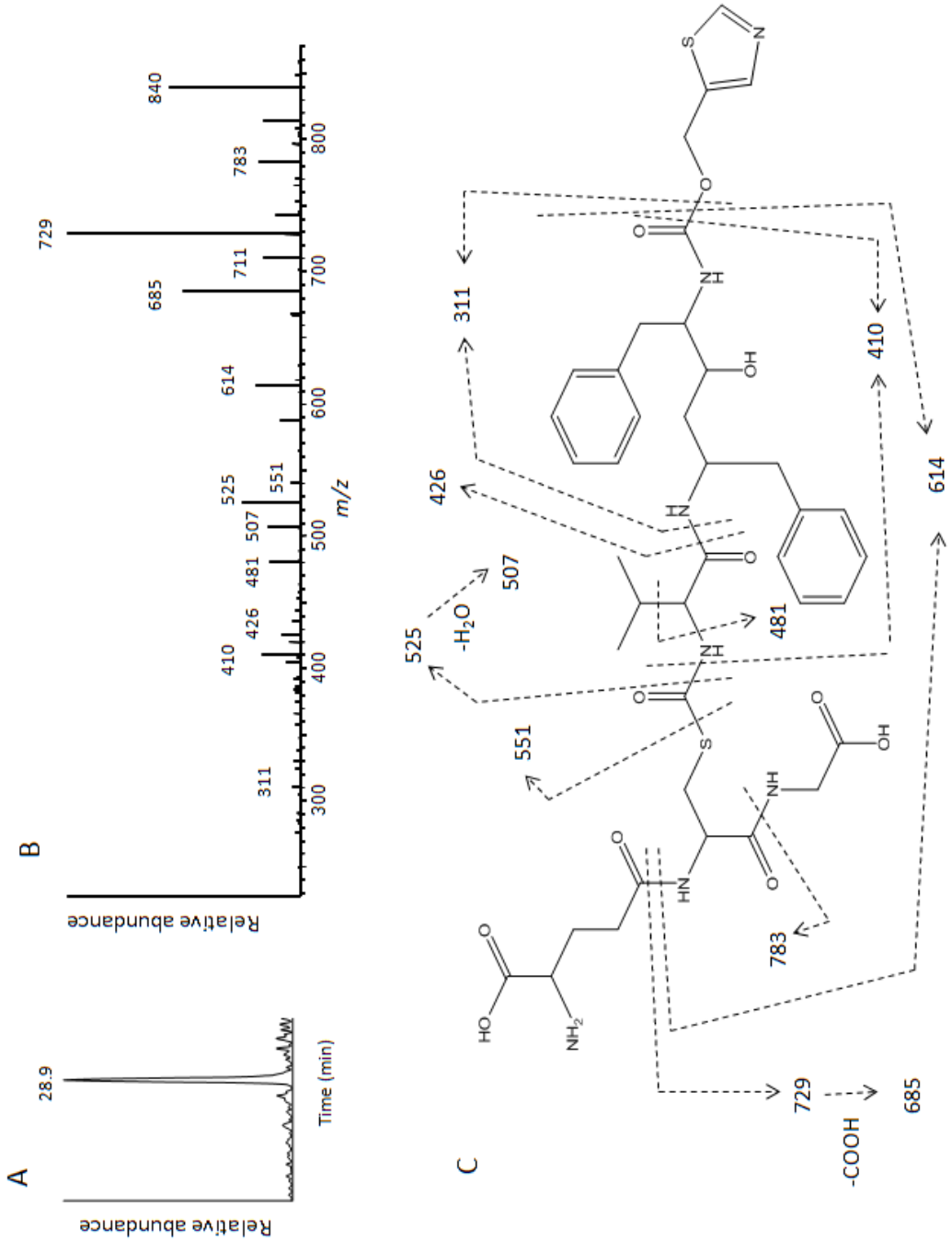

Fig. 10

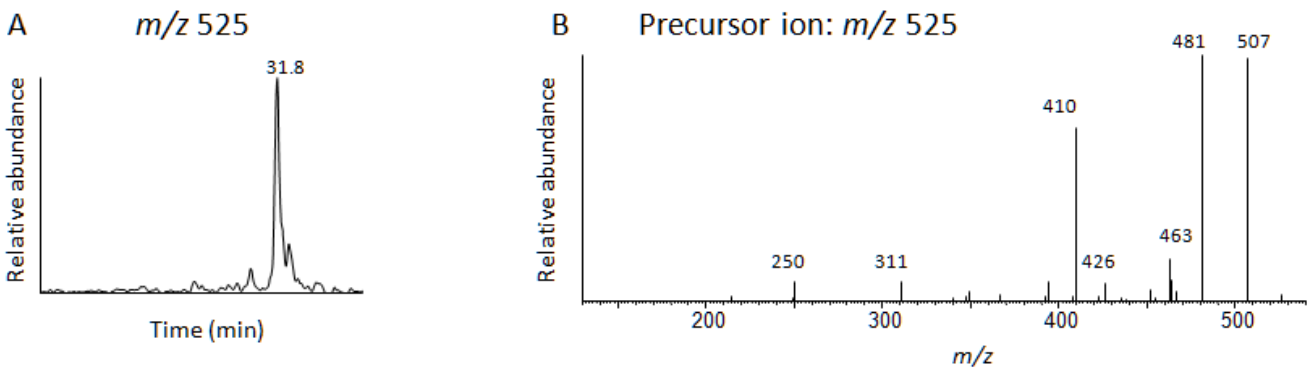

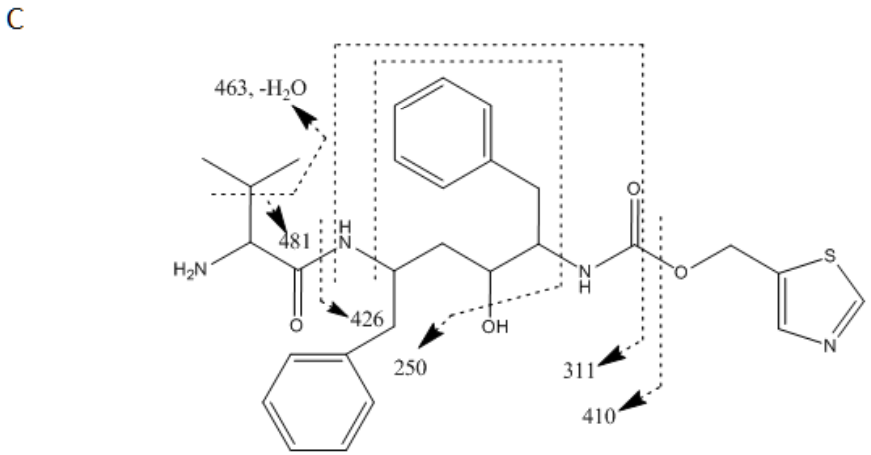

Fig. 11